

Numerical Simulation of Thermocapillary Pumping Using the Volume of Fluid Method

Feng C. Lai

School of Aerospace and Mechanical Engineering, University of Oklahoma, Norman, OK 73019

Carlos A. Sanchez

Riskmetrics Inc., Norman, OK 73071

Mauricio A. Sanchez

Department of Physics and Engineering, University of Central Oklahoma, Edmond, OK 73034

This report provides an initial study in thermocapillary induced flow in a microchannel through a two-dimensional volume of fluid model. A non-mechanical pumping mechanism, thermocapillary pumping (TCP), for moving a nL-sized drop within the channel is described. In TCP, one end of the drop is heated to create a surface tension difference between the ends of the drop resulting in drop motion. This numerical study assumes a constant motion of a liquid drop with constant contact angle. By inducing a strong temperature gradient of 50° C between the left end surface of the liquid drop and the channel walls, the drop attains continuous motion along the entire microchannel length. This motion results from varying surface tension forces acting at the two extreme ends of the liquid drop. © 2006 Oklahoma Academy of Science

INTRODUCTION

Micro-fabrication is touted as the new budding technology for miniaturization in applications, including the thermal management of electronic components and hand-held chemical analysis systems. Microfluidic systems are being developed to transport nano-sized volumes of liquids through miniaturized network assemblies. Applications for these devices include species separation, DNA sequencing, and combinatorial chemistry (Darhuber 2003). Micro-fabricated fluidic devices present many new engineering challenges in developing predictive capabilities for single-phase and multi-phase transport in micro passages (Gurrin 2002).

In bioengineering, there are problems in which the surface tension plays a major role. The best known example is the effect of surface tension between air and amniotic fluid on the ability of a newborn baby

catching its first breath (Huang 2001). The surface tension controls the inflation of the pulmonary alveoli. It has a major effect on pulmonary physiology.

The use of Micro-Electro-Mechanical Systems (MEMS) technology requires that the behavior of the molecule in the MEMS device is analogous to its behavior in a test tube. Specifically, several key relationships need distinctions that are more detailed. These include the effect of the velocity fields on the structural integrity of the molecule; the impact of non-Newtonian and viscoelastic properties of the fluid on the velocity fields; the surface interactions between the channel, the molecule, and the mechanisms used by the fluid to flow through the channel (Shrewsbury 1999). When modeling fluid flow through MEMS devices, details concerning extreme shear stress, surface-to-volume ratios, geometry changes, and property variation are of great importance for the analysis. Elucidating the mechanisms that

Proc. Okla. Acad. Sci. 86: pp 75-83 (2006)

govern biological microfluidic flow is not trivial. Classical theories require revision when applied to microfluidics. Although the fluid flow involved is usually laminar, in this low Reynolds number regime, effects that are traditionally ignored gain importance due to the similarity in scale between the macromolecule (droplet/bubble) and the MEMS channel.

Different transport mechanisms have been used in microfluidic devices, including pressure gradients, electrophoresis and electro-osmosis, electrohydrodynamics, magnetohydrodynamics, centrifugation, and thermocapillary pumping (TCP; Darhuber 2003). The TCP technique uses heating elements exterior to a closed channel to modify the surface tension at one end of a liquid plug. The difference in temperature between the front and back ends generates a capillary pressure gradient for liquid propulsion.

In this study, we will investigate the feasibility of actuating micro fluids through TCP in a temperature field with applications in the control of biofluid and drug delivery. For the flow regime, viscous forces usually dominate over inertial forces, and surface tension becomes a factor (Shrewsbury 1999). In pumping by interfacial tension, the surface tension of a droplet/bubble can be locally manipulated to achieve two different curvatures. Because the curvature is related to a specific pressure, a pressure difference within the droplet/bubble makes the droplet/bubble move.

This study will investigate how a temperature gradient may affect the flow in microchannels while TCP is also achieved. For the successful accomplishment of this proposal, a complete understanding of surface tension on the flow development (Li and Lai 2002, Li 2002) and the method to evaluate the numerical simulations (Hirt and Nichols 1981) is critical. Numerical model simulations will be conducted first. The proposed numerical model will be an improvement over the one recently reported by Gurrin et al (2002) to include the correct

Proc. Okla. Acad. Sci. 86: pp 75-83 (2006)

interface conditions and better treatment of a moving boundary for continuous drop motion. Because of the complexity of the model and significant computational efforts involved, the numerical calculations will be performed using Fluent®, Computational Fluid Dynamic (CFD) software suitable for this kind of project.

Below, we briefly describe the working principle of TCP. Also, the volume of fluid (VOF) formulation is detailed. The last parts of this paper detail the coupling of the method formulation with the flow solution and present the results for a drop of ink accelerated by a temperature field and a simple case with complete thermocapillary effect accounted for in a horizontal microchannel. The conclusions are presented at the end of the document.

THERMOCAPILLARY PUMPING DEVICE

Surface tension effect near the curved meniscus of a discrete drop results in a pressure jump across the liquid and gas phases. This jump is given by the Young-Laplace equation

$$P_g - P_l = \frac{G\sigma\cos\theta}{d} \quad (1)$$

where P_g and P_l represent the pressure on the gas and liquid side, respectively; σ is the surface tension; θ is the contact angle (Fig. 1); and d is the height of the channel. The factor G is a geometrical constant of the channel. For parallel plate channels $G = 2$. In a TCP device the receding interface of $L =$ drop length (m) liquid drop is heated. This causes a reduction in surface tension given by Li and Lai (2002)

$$\sigma = a - bT \quad (2)$$

where a and b are empirical constants.

For most of the liquids in the temperature range of interest, this linear law is applicable. The resulting TCP velocity,

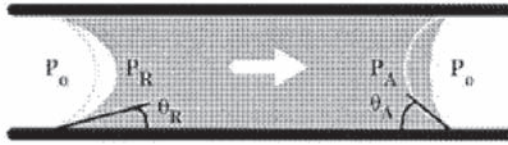


Figure 1. Discrete drop in a channel showing curved menisci (hydrophilic $\theta < 90^\circ$) at the drop ends.

separated from the heated zone, is based upon the net pressure difference across the liquid. This can be modeled as a Poiseuille flow in which the pressure difference induced is balanced by shear at a steady state (Sammarco 2000).

$$v = \frac{dGb\cos\theta_R}{LS\mu} \left[\Delta T - \left(\frac{a}{b} - T_A \right) \left(1 - \frac{\cos\theta_A}{\cos\theta_R} \right) \right] \quad (3)$$

where

$$\Delta T = T_A - T_R \quad (4)$$

and S is the channel shape constant, μ is the liquid dynamic viscosity, L is the drop length, and $T_{A,R}$ is the interface temperature with the subscript A referring to the advancing end of the moving drop and R referring to the receding end (left surface). As evident in (3), the TCP velocity is driven by the induced temperature difference ΔT between the ends of a single drop (Sammarco 2000).

VOLUME OF FLUID (VOF) METHOD

A large number of flows encountered in nature and technology are a mixture of phases. Physical phases of matter are gas, liquid, and solid, but the concept of phase in a multiphase flow system is applied in a broader sense. In multiphase flow, a phase can be defined as an identifiable class of material that has a particular inertial response to, and interaction with, the flow and the potential field in which it is immersed. For example, different-sized solid particles of the same material can be treated as different phases. Each collection of particles with the same size will have a similar dynamical response to the flow field (Fluent 2006).

The VOF model is a surface-tracking technique applied to a fixed Eulerian mesh domain. It is designed for two or more immiscible fluids where the position of the interface between the fluids is of interest. In the VOF model, a single set of momentum equations is shared by the fluids. The volume fraction of each of the fluids in each computational cell is tracked throughout the domain. Applications of the VOF model include stratified flows, free-surface flows, the steady or transient tracking of any liquid-gas interface, among others (Fluent 2006).

The VOF formulation relies on two or more fluids (or phases) not interpenetrating. For each additional phase added to the model, a variable is introduced: the volume fraction of the phase in the computational cell. In each control volume, the volume fractions of all phases sum to unity. The fields for all variables and properties are shared by the phases and represent volume-averaged values, as long as the volume fraction of each of the phases is known at each location. Thus the variables and properties in any given cell are either purely representative of one of the phases or representative of a mixture of the phases, depending upon the volume fraction values (Fluent 2006).

The tracking of the interface(s) between the phases is accomplished by the solution of a continuity equation for the volume fraction of one (or more) of the phases. For the q_{th} phase, this equation has the following form (Fluent 2006):

$$\frac{1}{\rho_q} \left[\frac{\partial}{\partial t} (\alpha_q \rho_q) + \nabla \cdot (\alpha_q \rho_q \vec{v}_q) \right] = \sum_{p=1}^n (m_{pq} - m_{qp}) \quad (5)$$

where m_{pq} is the mass transfer from phase q to phase p and m_{qp} is the mass transfer from phase p to phase q .

The volume fraction equation is not to be solved for the primary phase; the primary-phase volume fraction will be computed based on the following constraint:

$$\sum_{p=1}^n \alpha_p = 1 \quad (6)$$

Proc. Okla. Acad. Sci. 86: pp 75-83 (2006)

The properties appearing in the transport equations are determined by the presence of the component phases in each control volume. In a two-phase system, for example, if the phases are represented by the subscripts 1 and 2, and if the volume fraction of the second of these is being tracked, the density in each cell is given by

$$\rho = \alpha_2 \rho_2 + (1 - \alpha_2) \rho_1 \quad (7)$$

In general, for a multi-phase system, the volume-fraction-averaged density takes on the following form (Fluent 2006):

$$\rho = \sum \rho_q \alpha_q \quad (8)$$

All other properties (e.g., viscosity) are computed in this manner.

GOVERNING EQUATIONS FOR FLOW COUPLED WITH THE VOLUME OF FLUID METHOD

A single momentum equation is solved throughout the domain, and the resulting velocity field is shared among the phases. The momentum equation, shown below, is dependent on the volume fractions of all phases through the properties ρ and μ (Fluent 2006).

$$\frac{\partial}{\partial t} (\rho \vec{v}) + \nabla \cdot (\rho \vec{v} \vec{v}) = \nabla P + \nabla \cdot [\mu (\nabla \vec{v} + \nabla \vec{v}^T)] + \rho \vec{g} + \vec{F} \quad (9)$$

The energy equation, also shared among the phases, is shown below.

$$\frac{\partial}{\partial t} (\rho E) + \nabla \cdot (\vec{v} (\rho E + P)) = \nabla \cdot [k_{eff} \nabla T] + S_h \quad (10)$$

The VOF model treats energy, E , and temperature as mass-averaged variables

$$E = \frac{\sum_{q=1}^n \alpha_q \rho_q E_q}{\sum_{q=1}^n \alpha_q \rho_q} \quad (11)$$

where E_q for each phase is based on the specific heat of that phase and the shared temperature.

The properties ρ and k_{eff} (effective thermal conductivity) are shared by the phases. The source term, S_h , contains contributions from radiation, as well as any other volumetric heat sources (Fluent 2006).

As with the velocity field, the accuracy of the temperature near the interface is limited in cases where large temperature differences exist between the phases. Such problems also arise in cases where the properties vary by several orders of magnitude. For example, if a model includes liquid metal in combination with air, the conductivities of the materials can differ by as much as four orders of magnitude. Such large discrepancies in properties lead to equation sets with anisotropic coefficients, which in turn can lead to convergence and precision limitations.

The VOF model can also include the effects of surface tension along the interface between each pair of phases. The model can be augmented by the additional specification of the contact angles between the phases and the walls, which for the present study was set to 45° by specifying a wall adhesion angle (Brackbill 1992).

The importance of surface tension effects is determined based on the value of two dimensionless quantities (Fluent 2006): the Reynolds number, Re , and the capillary number, Ca ; or the Reynolds number, Re , and the Weber number, We . For $Re \ll 1$, the quantity of interest is the capillary number

$$Ca = \frac{\mu U}{\sigma} \quad (12)$$

and for $Re \gg 1$, the quantity of interest is the Weber number:

$$We = \frac{g L U^2}{\sigma} \quad (13)$$

where U is the free-stream velocity. Surface tension effects can be neglected if $Ca \gg 1$ or $We \gg 1$. For this project, the Reynolds

number Re is small, thus capillary effects are of great importance (Darhuber 2003, Darhuber 2005, Farahi 2005).

RESULTS

To compare the action of surface/capillary forces increasing the propulsion of a liquid drop, a known problem (Fluent Users, 2002) has been modified for this task. This simulation provides guidelines during the transient simulation of drop ejection from the nozzle of the printhead in an ink jet printer. The volume of filling is used to predict the droplet shape. To capture the capillary effect of the ejected ink, the surface tension and prescription of the wetting angle are specified. The surface inside the nozzle is neutrally wettable (contact angle = 175°), while the surface surrounding the nozzle orifice is non-wettable. At time zero, ink fills the nozzle. The rest of the domain is filled with air. Both fluids are assumed to be at rest. To initiate the ejection, the ink velocity at the inlet boundary suddenly rises from 0 to 1.8 m/s and drops according to a cosine law. After $10 \mu s$, the velocity returns to zero. The calculation is run more than the duration of the initial impulse.

The above problem is solved using Fluent, and screen shots of position are saved along the air channel. The problem is resolved by now including temperature along the channel. The air channel and ink compartment are initially at 293 K. To initiate the ejection, the ink velocity at the inlet boundary suddenly rises from 0 to 1.8 m/s and drops according to a cosine law. After $10 \mu s$, the velocity returns to zero. Also at 1 microsecond the temperature of one portion of the air channel wall ($L = 40 \mu m$) is increased to 343 K. The calculation is run

following the previous model. The surface tension varies according to equation 2.

The following results show the effects of adding temperature to the air chamber in comparison to the flow results at several time steps. Adobe Photoshop® has been used to merge the screen shots from both simulations. The white and black pixels represent the flow simulation, whereas the color represents the flow-temperature simulation.

Figure 2 shows the ink bubble away from the nozzle after the inlet velocity is turned off. Both simulations now produce different bubble shapes. The mean diameter is around $20 \mu m$. Due to temperature gradient the bubble from the second simulation is elongated due to enhancement of traveling speed. Due to stronger capillary forces, there is propulsion of the drop. The sequence of screen shots simply shows the difference between the two simulations and the enhancement of velocity by temperature gradient.

We have demonstrated that addressable heating mechanisms can be used to actuate and manipulate continuous streams or discrete drops of liquid. A numerical simulation for the flow speed of single liquid drops allows to be increased due to TCP effect.

Simulations to capture the physics of the flow encountered in TCP by differentially heating the liquid drop are captured. A $150 \mu m \times 25 \mu m$ channel was used with a movable heater simulating a sequence of heater arrays, prior to covering the left end of the liquid water drop. This microchannel was selected to match the results obtained by Gurrum et al (2002). The model is not grid dependent. For better visualization and accuracy of the simulations the chosen grid system for the channel was of 5104 quadri-

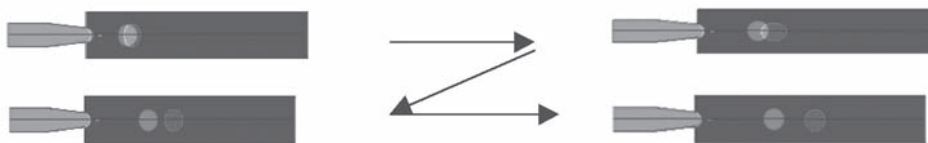


Figure 2. Volume fraction of ink bubble at different time steps.

lateral cells from which 1044 cells make the water drop.

The heater was maintained at a temperature of 80°C while the rest of the lower wall was fixed at 20°C (Gurruum 2002). The top and bottom walls are heaters. The length of the liquid drop along the centerline of the channel was 30 μm . Liquid density was taken as 1000 kg/m^3 and viscosity was assumed to be $1.1365 \times 10^{-3} \text{ N}/\text{m}^2\text{s}$.

Table 1 shows the temperature distribution in the channel for the above case after 20 μs . Even with a very low thermal conductivity value given for the liquid, there is a sufficient pressure and temperature gradient. Figure 3 shows the temperature distribution

Table 1. Temperature and pressure distribution of the liquid drop measured at one coordinate position along a vertical axis (Y) and at three positions on (X), showing the two surface ends and the middle of the drop at time 20 μs .

| X coord [μm] | Y coord [μm] | T [K] ¹ | P [Pa] ¹ |
|------------------------------|------------------------------|--------------------|---------------------|
| 25 | 25 | 351.49 | P = -1835.77 |
| 38 | 25 | 336.42 | P = -1920.11 |
| 62 | 25 | 294.07 | P = -1697.49 |

¹ T[K] = Temperature
P[Pa] = Pressure

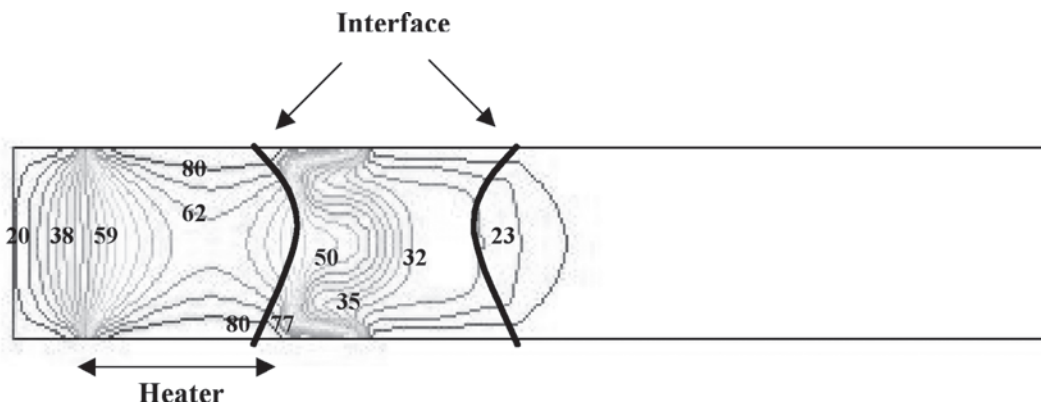


Figure 3. Temperature contours (in °C) after 68 μs . A gradient across the receding interface can be seen.

Proc. Okla. Acad. Sci. 86: pp 75-83 (2006)

in the channel for the above case after 68 μs . Even with a very low thermal conductivity value given for the liquid, there is a significant gradient across the receding interface.

Figure 4 plots the pressure along the position of the liquid drop at the top of the heater for different time steps. A gradient across the center and left end of the drop is seen along expected lines. As the drop attains hydrophilic position the pressure at the edge oscillates while the other remains fairly constant. The time response of the average speed of the drop is shown in Figure 5. The attained velocities are in agreement with those found by Gurruum et al (2002). In the beginning, the top edge of the left interface moves towards left due to temperature gradient across the interface. With the development of the temperature field, it returns back. This potentially explains the oscillatory behavior of the flow. It later diminishes as it advances along the channel. This may account for the strong surface shear stress at the wall.

Figure 6 shows the volumetric fraction of the liquid drop at different time steps. The effect of temperature gradient across the receding interface results in a net upward motion, causing deviation in the streamlines near the lower corner of the receding interface.

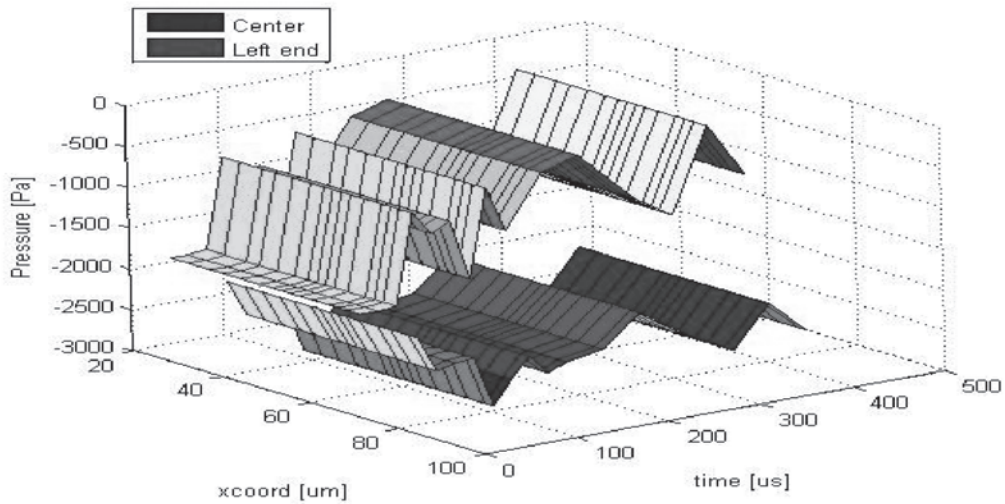


Figure 4. Pressure distribution between the left end of the drop and the center for different times. It can be seen that there is always an oscillating pressure gradient between the end and center of the drop. “xcoord” shows the distance between the left and center position for each time step.

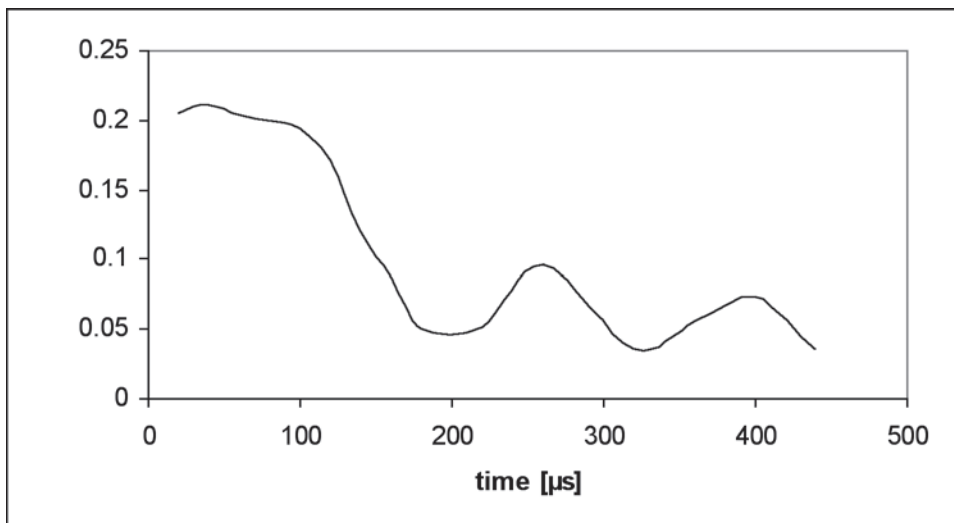


Figure 5. Average speed with time for thermocapillary flow. The flow is seen to be oscillatory.

CONCLUSIONS

We have studied thermocapillary flow generated by a constant thermal gradient along hydrophilic microchannel with constant width. The flow field in a discrete drop caused by a simple differential surface tension across the two interfaces of a liq-

uid drop in a microchannel was analyzed numerically by using the volume of fluid method.

The successful application of TCP is dependent upon the device’s ability to control the liquid temperatures at the menisci of the drop. The analysis carried out in the present work can be used as an efficient design

Proc. Okla. Acad. Sci. 86: pp 75-83 (2006)

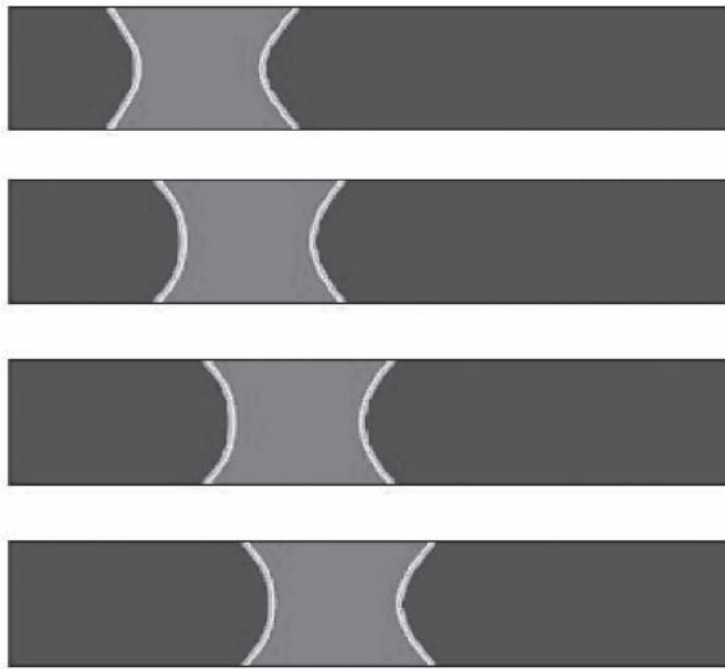


Figure 6. Volumetric fraction of liquid drop moving along the channel at different time steps.

tool and can be extended to microreaction systems. These results demonstrate the feasibility of thermocapillary flow as an actuation method for droplet-based microfluidic systems.

Additional research is necessary to get the heater walls to satisfy real engineering situations where a series of sequential microheater arrays can be set along the wall and attain continuous liquid motion. For possible medical use, a temperature of 80°C might destroy the cells making the biofluid, thus in order to reduce the heater temperature and attain similar fluid motion, the thermal conductivity of the fluid must be increased. The higher the thermal conductivity (a different fluid), the fastest period of time the thermocapillary effect is presented. Even though hydrophilic devices have been analyzed, the variation of contact angle with temperature is an issue that needs to be considered.

The results of this variation could cause the liquid drop to increase or decrease

speed and direction of motion. It is known that contact angle hysteresis reduces the temperature driving force of TCP. This hysteresis might produce bubble boiling before the bubble has an opportunity to start moving.

ACKNOWLEDGEMENTS

The authors acknowledge support for this work by NSF-EPSCoR Research Opportunity Award, monitored by Dr. Frank Waxman.

REFERENCES

- Brackbill JU, Kothe DB, Zemach C. 1992. A continuum method for modeling surface tension. *J Comput Phys* 100:335-354.
- Darhuber, AA, Troian SM. 2005. Principles of microfluidic actuation by modulation of surface stresses. *Ann Rev Fluid Mech* 37:425-455.
- Darhuber, AA, Valentino J, Davis JM, Troian SM. 2003. Microfluidic actuation by modulation of stresses. *Appl Phys Lett* 82:4:657-659.

- Darhuber AA, Davis JM, Troian, SM. 2003. Thermo-capillary actuation of liquid flow on chemically patterned surfaces. *Phys Fluids* 15:1295-1304.
- Farahi RH, Passian A, Ferreli TL, Thundat T. 2005. Marangoni forces created by surface plasmon decay. *Optic Lett* 30:6:618-618.
- Fluentusers.com. 2006. Fluent 6.2 Documentation Chapter 24: General multiphase methods [Online] Available from <http://www.fluentusers.com> (password protected). (Accessed 7 August 2006).
- Fluentusers.com. 2004. Tutorial: Drop ejection from a printhead nozzle [Online]. Available from <http://www.fluentusers.com>. (Accessed 9 January 2006).
- Gurram, S, Murthy S, Joshi Y. 2002. Numerical simulation of thermocapillary pumping using level set method. Proceedings of the 5th ISHMT/ASME Heat and Mass Transfer Conference; January 3-5, Kolkata, India.
- Hirt, CW, Nichols BD. 1981. Volume of fluid (VOF) method for the dynamics of free boundaries. *J Comput Phys* 39:201-225.
- Huang W, Bhullar RS, Fung YC. 2001. The surface-tension-driven flow of blood from a droplet into a capillary tube. *Trans ASME* 123:446-454.
- Li CT, Lai FC. 2002. Effects of gravitation and surface tension on flow injection in center-gated disks. AIAA 40th Aerospace Sciences Meeting, AIAA Paper 2002-0760 7p.
- Li, CT. 2002. Numerical study of surface tension and gravitational effects on mold filling. [Ph.D. Dissertation], Norman (OK): University of Oklahoma. Available from: University of Oklahoma Library.
- Sammarco TS, Burns MA. 2000. Heat transfer analysis of microfabricated thermocapillary pumping and reaction devices. *J Micro Mech Micro Eng* 10:42-55.
- Shrewsbury PJ, Muller SJ, Liepmann D. 1999. Characterization of DNA flow through microchannels. In: Technical Proceedings of The 1999 International Conference on Modeling and Simulation of Microsystems: Chpt. 16; Applications: Microfluids [online]. Puerto Rico, 19-21 April 1999. Available from: <http://www.nsti.org/proc/msm99>.

Received: April 21, 2006; Accepted August 1, 2006.